International Journal of Mechanical, Industrial and Aerospace Sciences
ISSN: 2517-9950
Vol:9, No:6, 2015

Prediction of Unsteady Forced Convection over Square Cylinder in the Presence of Nanofluid by Using ANN

Ajoy Kumar Das, Prasenjit Dey

***Abstract*—**Heat transfer due to forced convection of copper water based nanofluid has been predicted by Artificial Neural network (ANN). The present nanofluid is formed by mixing copper nanoparticles in water and the volume fractions are considered here are 0% to 15% and the Reynolds number are kept constant at 100. The back propagation algorithm is used to train the network. The present ANN is trained by the input and output data which has been obtained from the numerical simulation, performed in finite volume based Computational Fluid Dynamics (CFD) commercial software Ansys Fluent. The numerical simulation based results are compared with the back propagation based ANN results. It is found that the forced convection heat transfer of water based nanofluid can be predicted correctly by ANN. It is also observed that the back propagation ANN can predict the heat transfer characteristics of nanofluid very quickly compared to standard CFD method.

***Keywords*—**Forced convection, Square cylinder, nanofluid, neural network.

I. Introduction

THE flow and heat transfer around slender cylindrical bluff bodies has been the subject of intense research, mainly owing to the tremendous engineering significance on heat exchangers, solar heating systems, natural circulation boilers, nuclear reactors, dry cooling towers, electronic cooling, vortex flow meters and flow dividers, probes, sensors and many more.

By using different methods, such as expanding the effective heat transfer area or heat transfer coefficient, convective heat transfer can be moderated. In recent, a modern class of fluid, called nanofluid, is developed and is using to enhance the heat transfer.

It is observed that thermal conductivity of nanofluid is higher than that of the base fluids when the nanoparticles are mixed in small amount [1], [2]. The application of nanofluid in convection for different industrial purpose is introduced in preceding studies [3], [4]. Recently, application of nanofluid on enhancement of heat transfer has studied [5], [6].

Various numerical and experimental studies of heat transfer characteristics by utilizing nanofluids has been studied and concluded in the literature [7], [8]. The heat transfer performance of nanofluids in a differentially heated enclosure and concluded that there is enhancement in heat transfer rate due to the mixing of nanoparticles in the base fluid is investigated [7]. Dey and Das [9] also studied the natural convection heat transfer inside a square enclosure with a heated square cylinder. Effect of different nanofluid, as Al2O3, CuO with water as base fluid & ethylene glycol and water mixture on momentum & forced convection (laminar and steady) over square cylinder has been studied recently [10] with different Pr. up to volume fraction 4% and they also make conclusion that there is an optimum value of volume fraction at a certain particle diameter.

Although, all the heat transfer studies are based on experimentally or numerically; but over the last few years, prediction of different characteristics of heat transfer and aerodynamic behavior are becoming an area of research in various engineering applications due to its less time consuming method. There are various techniques are using in prediction; between them Artificial Neural Network (ANN) is one of the most utilizing method. Recently, [11] studied the prediction of heat transfer in the presence of nanofluid using ANN and found that ANN can be used to predict heat transfer characteristics most efficiently and rapidly.

By considering the forgoing studies, it is altogether okay to conclude that there is no prior study has been conducted on prediction of nanofluid based convection over a square cylinder. Therefore, in the present study, the prediction of unsteady forced convection by utilizing nanofluid is studied by back propagation ANN. The Reynolds number are kept at 100 and solid volume fraction as 0 to 15%.

II. Model Description and Governing Equations

The system of interest here is to predict the forced convection heat transfer characteristics past over a square cylinder in a channel at the symmetric horizontal line, schematically shown in Fig. 1. The square cylinder of depth D with constant wall temperature T_w is held in a channel subjected to an upstream steady laminar flow of x-velocity, $u = u_\infty$ (free stream velocity) and temperature, T_∞. The aim is to simulate an infinitely long channel; however, the computational domain has to be finite. The distance of the upstream and the downstream boundaries from the center of the cylinder are L_u=10D and L_d=40D. The distance between the upper and lower side-walls, H, is specified according the blockage ratio (D/H=0.05). The no slip boundary condition is associated with the side-walls.

Ajoy Kumar Das, Associate Professor, is with the Mechanical Engineering Department, National Institute of Technology Agartala, India e-mail: akdas_72@yahoo.com, Fax: 91-0381-2346360.

Prasenjit Dey, Ph.D Scholar, is with the Mechanical Engineering Department, National Institute of Technology Agartala, India (e–mail: prasenjitmit1@gmail.com).

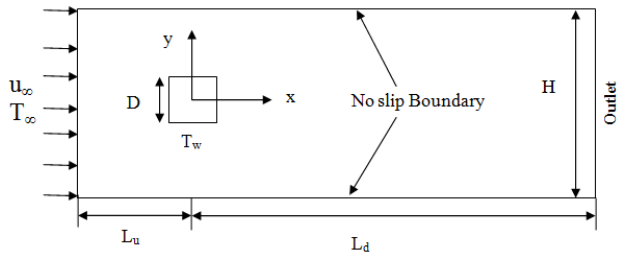

Fig. 1 A schematic diagram of the problem description

A. Governing Equations

The dimensionless governing equations for the two dimensional, laminar, incompressible nanofluid flow and heat transfer with constant thermo-physical properties and negligible dissipation effect can be expressed in the following forms:

$$\frac{\partial u}{\partial x}+\frac{\partial v}{\partial y}=0 \tag{1}$$

$$\frac{\partial u}{\partial t}+u\frac{\partial u}{\partial x}+v\frac{\partial u}{\partial y}=-\frac{\rho_f}{\rho_{nf}}\frac{\partial p}{\partial x}+\frac{\mu_{eff}}{\nu_f\rho_{nf}}\frac{1}{\mathrm{Re}}\left(\frac{\partial^2 u}{\partial x^2}+\frac{\partial^2 u}{\partial y^2}\right) \tag{2}$$

$$\frac{\partial v}{\partial t}+u\frac{\partial v}{\partial x}+v\frac{\partial v}{\partial y}=-\frac{\rho_f}{\rho_{nf}}\frac{\partial p}{\partial y}+\frac{\mu_{eff}}{\nu_f\rho_{nf}}\frac{1}{\mathrm{Re}}\left(\frac{\partial^2 v}{\partial x^2}+\frac{\partial^2 v}{\partial y^2}\right)+\frac{\rho_p\beta_p\phi+\rho_f\beta_f(1-\phi)}{\rho_{nf}\beta_f}Ri(T) \tag{3}$$

$$\frac{\partial \theta}{\partial t}+u\frac{\partial \theta}{\partial x}+v\frac{\partial \theta}{\partial y}=\frac{\alpha_{nf}}{\alpha_f}\frac{1}{\mathrm{RePr}}\left(\frac{\partial^2 \theta}{\partial x^2}+\frac{\partial^2 \theta}{\partial y^2}\right) \tag{4}$$

where u, v are the dimensionless velocity components along x and y directions of a Cartesian coordinate system respectively, p is the dimensionless pressure, Re $\left(=\frac{\rho_f u_\infty D}{\mu_f}\right)$ is the Reynolds number based on the cylinder dimension, θ is the dimensionless temperature, Pr $\left(=\frac{\mu_f C_{pf}}{K_f}\right)$ is the Prandtl number and t is the dimensionless time. The fluid properties are described by the density ρ, kinematic viscosity μ and thermal conductivity k. The dimensionless variables are defined as:

$$u=\frac{\bar{u}}{u_\infty},\ v=\frac{\bar{v}}{v_\infty},\ x=\frac{\bar{x}}{D},\ y=\frac{\bar{y}}{D},\ \theta=\frac{T-T_\infty}{T_w-T_\infty} \tag{5}$$

$$t=\frac{u_\infty \bar{t}}{D}$$

B. Thermophysical Properties of Nanofluid

The different thermophysical properties of nanofluid are defined as:

$$\mu_{nf}=\frac{\mu_f}{(1-\phi)^{2.5}} \tag{6}$$

$$\rho_{nf}=(1-\phi)\rho_f+\phi\rho_p \tag{7}$$

$$C_{pnf}=\frac{(1-\phi)(\rho C_p)_f+\phi(\rho C_p)_p}{\rho_{nf}} \tag{8}$$

$$\frac{k_{nf}}{k_f}=\frac{(k_p+2k_f)-2\phi(k_f-k_p)}{(k_p+2k_f)+\phi(k_f-k_p)} \tag{9}$$

The thermophysical properties of fluid and nanoparticles are given in Table I [12].

TABLE I
THERMOPHYSICAL PROPERTIES OF NANOFLUID

Fluid/ Nanoparticle	Thermophysical properties			
	ρ	Cp	k	μ
Water	997.1	4179	0.613	0.001
Cu	8933	385	400	_

C. Boundary Conditions

The physical boundary condition for the above discussed problem configuration are written as follows:

- The left wall of the computational domain is designed as the inlet. The "velocity inlet" boundary condition is assigned at the inlet boundary with free stream velocity, u_∞, temperature T and Neumann boundary condition for pressure is used $\left(\frac{\partial p}{\partial x}=0\right)$.
- The usual no-slip boundary condition is assigned for flow at the surface of the cylinder, i.e. u=0; v=0 with constant wall temperature of θ=1 and normal gradient condition for pressure $\left(\nabla p.\hat{n}=0, where\ \hat{n}\ is\ the\ unit\ normal\right)$
- Towing-tank boundary condition is assigned at the upper and lower surface of the computational domain, i.e. $u=u_\infty$: v=0.
- The extreme right surface of the computational domain is assigned as outlet. The "pressure outlet" boundary condition is employed at the exit boundary with a fully developed flow situation $\left(\frac{\partial u}{\partial x}=0,\frac{\partial v}{\partial x}=0,\frac{\partial \theta}{\partial x}=0\right)$ of Dirichlet type Pressure boundary condition (p=0).

III. NUMERICAL DETAILS

In the present investigation, the numerical simulation is performed by using the finite volume based commercial CFD solver Ansys FLUENT. FLUENT is used to solve the governing equations which are the partial differential equations, using the control volume based technique in a collected grid system. The solver used in the present work is pressure-based implicit method. Semi-Implicit Method for Pressure-Linked Equation (SIMPLE) is selected for the pressure-velocity coupling scheme. The pressure term is discretized under the scheme of STANDARD whereas the momentum is discretized by second order upwind scheme. The laminar viscous model is used for the low Reynolds number consideration. The convergence criteria for the continuity and velocity are set to 10^{-5}.

The heat transfer characteristic between the cylinder and the surrounding fluid is calculated by the Nusselt number. The local Nusselt number and the Stanton number based on the cylinder dimension is given by:

$$Nu = \frac{hD}{k} = -\frac{\partial \theta}{\partial n} \quad (10)$$

where, h is the local heat transfer coefficient, k is the thermal conductivity of the fluid and n is the direction normal to the cylinder surface. Surface average heat transfer is obtained by integrating the local Nusselt number along the cylinder face. The time average Nusselt number is computed by integrating the local value over a large time period.

IV. Artificial Neural Network Model

Artificial neural network (ANN) is a computational structure inspired by a biological neural system. An ANN consists of very simple and highly interconnected units called neurons. The neurons are connected to each other by links in which individual weights are passed and over which signals can pass. The arrangement of neurons into layer and the connection pattern within and between the layers are called as network architecture. Each neuron receives multiple inputs from other neurons in proportion to their connection weights and generates a single output, which may be propagated to several other neurons [13].

A single artificial neuron can be implemented in many different ways. The general mathematic formulation of a single artificial neuron could be defined as:

$$y(x) = f\left(\sum_{i=0}^{n} w_i x_i + b\right) \quad (11)$$

where, x is a neuron with n input (x_0 to x_n) and one output y(x) and where (w_i) are weights determining how much the inputs should be weighted with b denoting the bias [14]. '*f*' is an activation function that weights how powerful the output should be from the neuron, based on the sum of the inputs and expressed as:

$$f(x) = \frac{1}{1+e^{-x}} \quad (12)$$

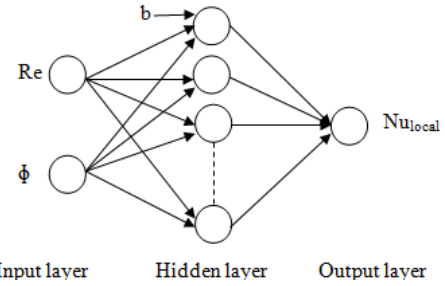

Fig. 2 Schematic representation of a multilayer feedforward network consisting of three inputs, one hidden layer with five neurons and three outputs

The basic feedforward network performs a non-linear transformation of input data in order to approximate the output data. In a multilayer feedforward ANN, the neurons are ordered in layers, starting with an input layer and ending with an output layer. Between these two layers, there are a number of hidden layers. For the present ANN model, three layers are used namely one input layer, one hidden layer and one output layer. Connections in these kinds of network only go forward from one layer to the next where all the neurons in each layer are connected to all the neurons in the next layer. The designed neural networks structure 2-10-1 (2 neurons in input layer, 10 neurons in hidden layer and 1 neurons in output layer) of the present study is shown in Fig. 2.

A. Training ANN

The back-propagation method is the most popular training algorithm. The input and output data are trained in ANN so that the weights can be adjusted to give the same outputs as found in the training data. The inputs (x) into a neuron are multiplied by their corresponding connection a weight (W), summed together and bias is added to the sum. This sum is transformed through a transfer function (*f*) to produce the required output, which may be passed to other neurons. After propagating an input through the network, the error is calculated and the error is propagated back through the network while the weights are adjusted in order to make the error smaller. The number of iterations 500 is selected for the present network. The training data has been selected 70% of the total data and the remaining data are selected for testing. Neural network requires that the range of the both input and output values should between 0.1 and 0.9 due to the restriction of sigmoid function. Therefore, the numerical data evaluated in this study are normalized by:

$$x_n = \left(\frac{x_i - x_{\min}}{x_{\max} - x_{\min}}\right) \quad (13)$$

where X_n = normalized value, X_i = actual input (or output) value, X_{max} =Maximum value of the inputs (or outputs), X_{min} =Minimum value of the inputs (or outputs).

V. Results and Discussions

A. Grid Testing and Validation of Present Results

In this study, three different mesh sizes (Grid1-15000, Grid2-25000 and Grid3-40000) are adopted in order to check the mesh independency (refer Fig. 3). A detailed grid independency study has been performed and results are obtained for the average Nusselt number at ϕ=0.0 but there is no considerable changes between Grid2 and Grid3 (refer Table II). Thus a grid size 25000 is found to meet the requirements of the both grid independency and computation time limit.

The present numerical data are validated with the available published data. The present data are validated for Pr=0.7 (Air) and Re=100. Number of trials has been performed to find quite accurate value and time step is chosen for every case as 0.01. The parameters used for validation are C_d, Cl_{rms} and Nu_{avg}. The present data are in very good agreement with the published data, tabulated in Table III.

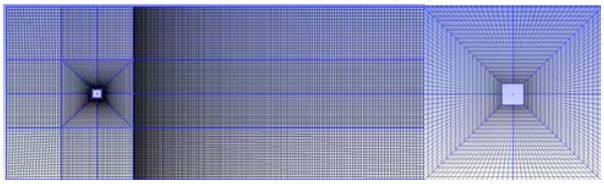

(a) (b)

Fig. 3 Grid Distribution of the computational domain (a), Zoomed view of the grid distribution of the cylinder (b)

TABLE II
STUDY OF EFFECT OF GRID SIZE FOR GRID INDEPENDENCY TEST

Number of cells	Re=100 Nu_{avg}
15000	6.700028
25000	6.871824
40000	6.902747

TABLE III
COMPARISON OF PRESENT NUMERICAL DATA WITH THE LITERATURE DATA

Source	Square cylinder		
	C_d	Cl_{rms}	Nu_{avg}
Present Study	1.5299	0.1698	3.8443
Sahu et. al [15]	1.4878	0.1880	4.0254

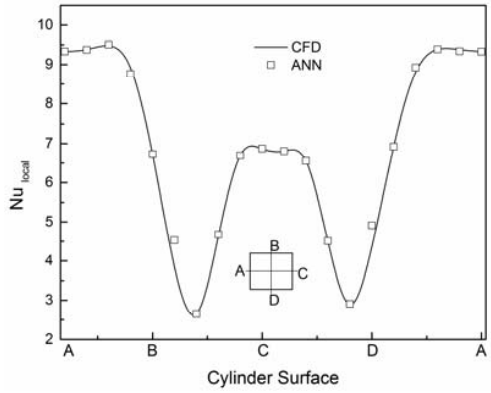

(a)

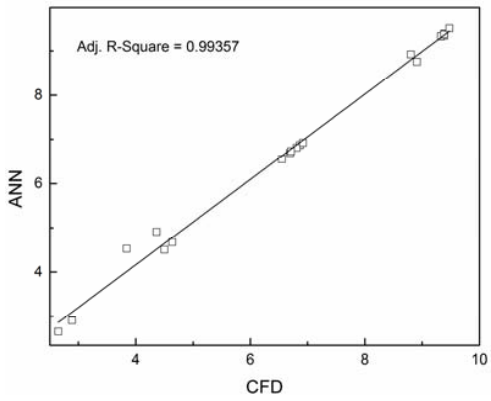

(b)

Fig. 4 Nu_{local} prediction over cylinder surface & (a), fitting plot of numerical & predicted data at ϕ=0.00 (b)

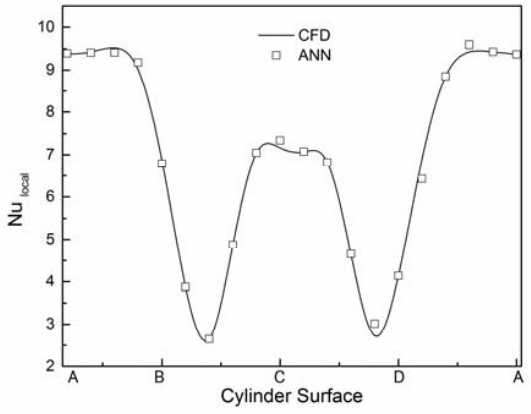

(a)

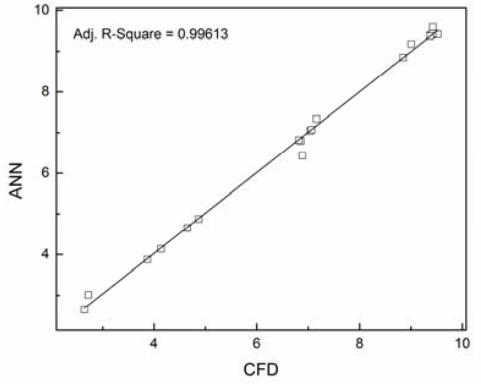

(b)

Fig. 5 (a) Nu_{local} prediction over cylinder surface & (b) fitting plot of numerical & predicted data at ϕ=0.03

B. Prediction of Heat Transfer

The heat transfer characteristic over the square cylinder due to presence of nanofluid is presented by means of local and average Nusselt number. At front stagnation point, the heat transfer is maximum due to the more clustering of isotherm lines & afterward it is decreasing gradually to the rear face of the cylinder. It is seen that there is gradual decrease and afterwards increase in Nusselt number at a point, which is the point of separation (refer Figs. 4 (a)–8 (a)). This kind of nature is found due to the presence of vortex in that region and continues to the rear separation point. It is found that by increasing of solid volume fraction, heat transfer rate is increased. As by increasing the solid volume fraction, the volume of nanoparticles striking the cylinder is increased, which causes more heat transfer from cylinder surface, by means of which the heat transfer rate is also increased. The training and testing data are collected from numerical analysis for Re= 100, ϕ= 0 to 15%. The training data are separated from the total data by keeping the particular testing data alongside. For training the network, different combinations of solid volume fraction are selected. For training the present ANN model, Reynolds number and volume fraction have taken as input and local Nusselt number is found as output. Figs. 4 (b)-8 (b) show the variation of numerical and predicted

data after testing the network, which are clearly depicted that the predicted data are in good agreement with the numerical data for every volume fraction.

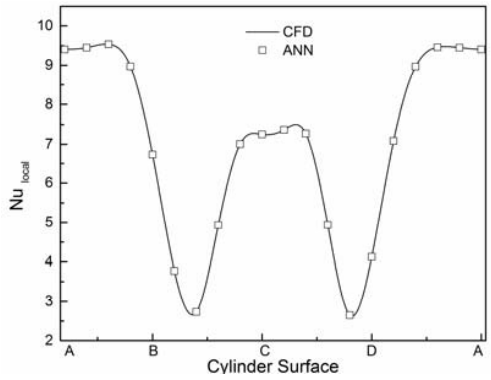

(a)

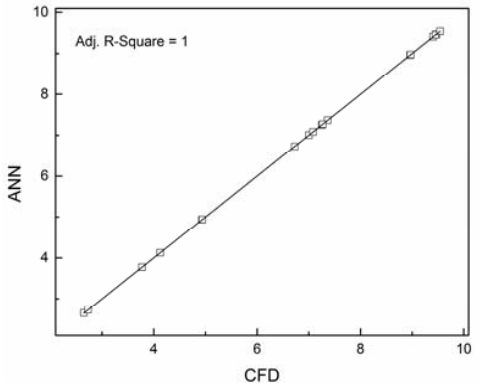

(b)

Fig. 6 Nu_{local} prediction over cylinder surface & (a), fitting plot of numerical & predicted data at ϕ=0.05 (b)

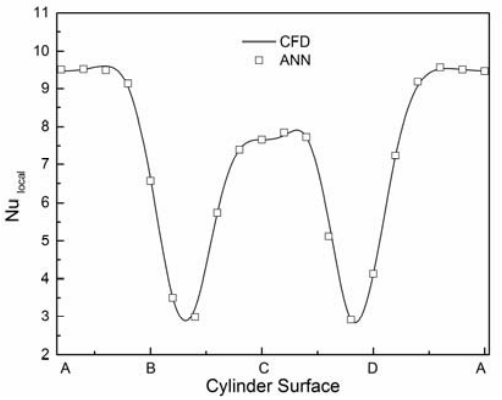

(a)

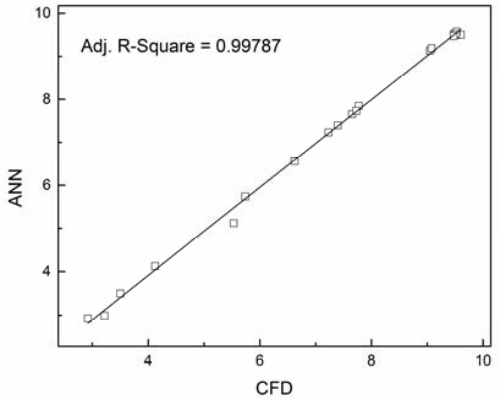

(b)

Fig. 7 Nu_{local} prediction over cylinder surface & (a), fitting plot of numerical & predicted data at ϕ=0.10 (b)

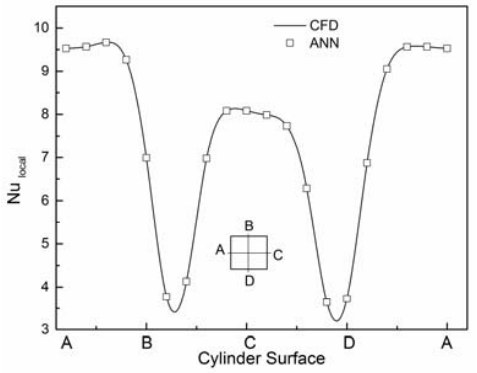

(a)

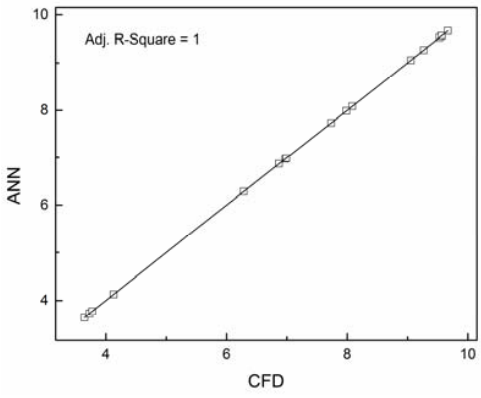

(b)

Fig. 8 Nu_{local} prediction over cylinder surface & (a), fitting plot of numerical & predicted data at ϕ=0.15 (b)

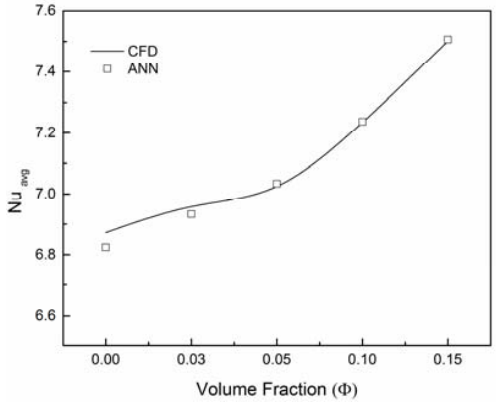

Fig. 9 Average Nusselt number prediction over cylinder

The average Nusselt number over the cylinder surface is also predicted in this present study. The variation of average Nusselt number about the cylinder surface is shown in Fig. 9 for Re=100 & ϕ=0.00 to 0.15. Only one case or Re is considered for predicting the local & average Nusselt number and it shows that a very good agreement between the numerical data and the predicted data. Hence, the present ANN model can be implemented for predicting the forced convection over square cylinder at different Re to minimize the computational time.

The error between the numerical values and the ANN predicted values are presented as Adjusted R^2 which is expressed as:

$$\bar{R}^2 = 1 - \frac{\sum_i (N_i - P_i)^2 \Big/ n - p - 1}{\sum_i \left(N_i - \bar{N}\right)^2 \Big/ n - 1} \tag{14}$$

where, n=Sample Size, p=total number of regressors in the training model. N_i= Actual Value. P_i=Predicted Value and $\bar{N} = \frac{1}{n}\sum_{i=1}^{n} N_i$

It is found that the maximum error in local Nusselt number is 0.643% for ϕ=0.00. It is obvious for ANN that, more values in training, more accurate will be the prediction.

The heat transfer over square cylinder is enhanced by introducing the nanoparticle at different volume fraction which is encapsulated in Table IV.

TABLE IV
% INCREMENT OF NU_{AVG} FOR DIFFERENT ϕ

ϕ	Nu_{avg}	% increment
0.00	6.871824	
0.03	6.957886	1.252389
0.05	7.025581	2.237499
0.10	7.234203	5.273403
0.15	7.501226	9.159169

VI. CONCLUSION

Back propagation Artificial Neural Network is used to predict the forced convection heat transfer characteristics of water based nanofluid flowing over a square cylinder at low unsteady Reynolds number. For this purpose, series of numerical data has been developed for the cylinder model with a validation which shows a very good agreement of present result with the previously available published data. For training and testing the network, several numerical cases with combinations of input variables are created and output data are generated. The validity of the applied predicted methods was investigated in several cases to ensure the effectiveness to establish the results with less permissible error. It can be concluded by analyzing the results that the present back propagation artificial neural network (2-10-1) can predict the local and average Nusselt number accurately with minimum mean relative error; hence reducing the computational time in CFD calculation while achieving acceptable accuracy.

REFERENCES

[1] Eastman, J. A., Choi, S. U. S., Li, S., Yu, W., & Thompson, L. J. (2001). Anomalously increased effective thermal conductivities of ethylene glycol-based nanofluids containing copper nanoparticles. *Applied Physics Letters*, *78*(6), 718-720.

[2] Xuan, Y., & Li, Q. (2000). Heat transfer enhancement of nanofluids. *International Journal of Heat and Fluid Flow*, *21*(1), 58-64.

[3] Buongiorno, J. (2006). Convective transport in nanofluids. *Journal of Heat Transfer*, *128*(3), 240-250.

[4] Kakaç, S., & Pramuanjaroenkij, A. (2009). Review of convective heat transfer enhancement with nanofluids. *International Journal of Heat and Mass Transfer*, *52*(13), 3187-3196.

[5] Daungthongsuk, W., & Wongwises, S. (2007). A critical review of convective heat transfer of nanofluids. *Renewable and Sustainable Energy Reviews*, *11*(5), 797-817.

[6] Trisaksri, V., & Wongwises, S. (2007). Critical review of heat transfer characteristics of nanofluids. *Renewable and Sustainable Energy Reviews*, *11*(3), 512-523.

[7] Khanafer, K., Vafai, K., & Lightstone, M. (2003). Buoyancy-driven heat transfer enhancement in a two-dimensional enclosure utilizing nanofluids. *International Journal of Heat and Mass Transfer*, *46*(19), 3639-3653.

[8] Tiwari, R. K., & Das, M. K. (2007). Heat transfer augmentation in a two-sided lid-driven differentially heated square cavity utilizing nanofluids. *International Journal of Heat and Mass Transfer*, *50*(9), 2002-2018.

[9] Dey, P., & Das, A. K. (2014, January). Numerical analysis of characteristic of flow and heat transfer due to natural convection in a enclosure (square) using nano-fluid. In *Advances in Energy Conversion Technologies (ICAECT), 2014 International Conference on* (pp. 92-98). IEEE.

[10] Vahid Etminan-Farooji, Ehsan Ebrahimnia-Bajestan, Hamid Niazmand, Somchai Wongwises. (2012). Unconfined laminar nanofluid flow and heat transfer around a square cylinder. *International Journal of Heat and Mass Transfer, 55,* 1475–1485

[11] Santra, A. K., Chakraborty, N., & Sen, S. (2009). Prediction of heat transfer due to presence of copper–water nanofluid using resilient-propagation neural network. *International Journal of Thermal Sciences*, *48*(7), 1311-1318.

[12] Abu-Nada, E., & Oztop, H. F. (2009). Effects of inclination angle on natural convection in enclosures filled with Cu–water nanofluid. *International Journal of Heat and Fluid Flow*, *30*(4), 669-678.

[13] Sreekanth, S., Ramaswamy, H. S., Sablani, S. S., & Prasher, S. O. (1999). A neural network approach for evaluation of surface heat transfer coefficient. *Journal of food processing and preservation*, *23*(4), 329-348.

[14] Kurtulus, D. F. (2009). Ability to forecast unsteady aerodynamic forces of flapping airfoils by artificial neural network. *Neural Computing and Applications*, *18*(4), 359-368.

[15] Sahu, A. K., Chhabra, R. P., & Eswaran, V. (2009). Effects of Reynolds and Prandtl numbers on heat transfer from a square cylinder in the unsteady flow regime. *International Journal of Heat and Mass Transfer*, *52*(3), 839-850.